Use of Organo- and Alkoxysilanes in the Synthesis of Grafted and Pristine Clays

Kathleen A. Carrado,*,† Langqiu Xu,†,‡ Roseann Csencsits,§ and John V. Muntean†

Chemistry and Materials Science Divisions, Argonne National Laboratory, Argonne, Illinois 60439

Received January 31, 2001. Revised Manuscript Received July 20, 2001

A one-step, direct method is described for the creation of synthetic smectite clays grafted with organics on the interlayer surfaces using an organotrialkoxysilane as the silica source. The silane employed most successfully is phenyltriethoxysilane (PTES). Aqueous slurries of LiF, magnesium hydroxide, and the silane are refluxed for 2−5 days, and desirable molar compositions are determined. X-ray powder diffraction, thermal analysis, IR, TEM, N_2 sorption isotherms, and solid-state ^{13}C and ^{29}Si NMR techniques are used to characterize the products. The loading of organics on the PTES−hectorites is determined at 20−25% and is comprised of phenyl groups as Si−C linkages. Evidence of this linkage includes an IR peak at 1430 cm^{-1} and ^{29}Si NMR assignments at −79 and −66 ppm for $RSi(OMg)(OSi)_2$ and RSi(OMg)(OSi)(OH) species, respectively. The use of tetraethoxysilane (TEOS) resulted in a pure hectorite and comprises the first report of the successful use of a tetraalkoxysilane silicon source for crystallizing hectorite from an aqueous solution.

Introduction

Recently a one-step, direct synthesis of covalently linked inorganic−organic lamellar nanocomposites based on the neutral clay talc structure was described.[1] Various organotrialkoxysilanes were employed to produce layered organo−clay structures with organophilic molecules covalently attached to the silicate interlayer surfaces.[1,2] Adding framework charge to the inorganic component has now enhanced this realm of unique organo−clay nanocomposite materials. In other words, smectite (swelling phyllosilicate) clays have been created in lieu of the neutral talc. The uncharged endmember of the 2:1 trioctahedral magnesium phyllosilicate series is talc, with a structure of $[Si_8Mg_6O_{20}(OH)_4]$. With some isomorphous substitution of Li(I) for Mg(II) in the central octahedral layer (see Figure 1), the mineral hectorite is formed. With an ideal composition of $[Ex_{.66}Si_8(Mg_{5.34}Li_{.66})O_{20}(OH,F)_4]$, where Ex = exchangeable cation, hectorite has a cation exchange capacity (cec) of about 80 mequiv/100 g.[3,4] The capabilities of swelling, high cec, and high surface area (80 m^2/gm) are similar to the analogous aluminosilicate montmorillonite mineral, and both clays have wide applications in catalysis, ion exchange, and adsorption.[5]

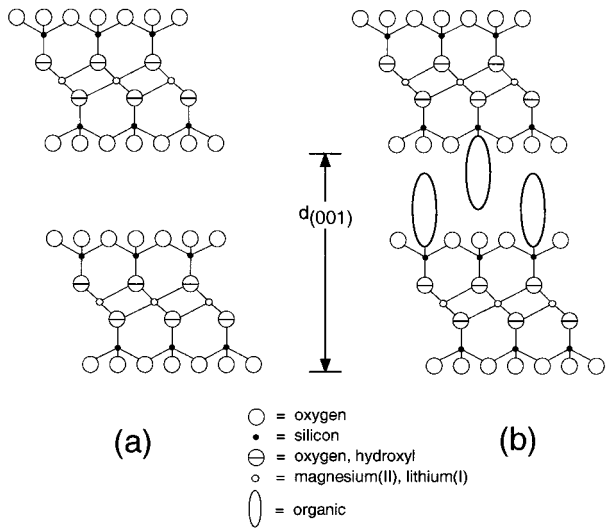

Figure 1. (010) view of 2:1 magnesium silicate hectorite clay structure in (a) inorganic form and (b) an organo-grafted form (only 1/2 Si atoms grafted in this example). Interlayer cations and water molecules are not shown. Two tetrahedral silicate layers are condensed to a central metal octahedral layer (shown here in projection).

One other report of using organoalkoxysilanes during clay synthesis describes the condensation of a copper-containing kaolinite clay mimic in the presence of (mercaptopropyl)trialkoxysilane.[6] However, kaolinite is not a smectite but a 1:1, nonswelling clay. Other than the reports of direct synthesis mentioned, the only other

* Author to whom all correspondence should be sent. Phone: (630)-252-7968. E-mail: kcarrado@anl.gov.
† Chemistry Division.
‡ Present address: PPG Industries, Inc., 4325 Rosanna Drive, Allison Park, PA 15101.
§ Materials Science Division.

(1) (a) da Fonseca, M. G.; Barone, J. S.; Airoldi, C. *Clays Clay Miner.* **2000**, *48*, 638 (b) Whilton, N. T.; Burkett, S. L.; Mann, S. *J. Mater. Chem.* **1998**, *8*, 1927.
(2) (a) da Fonseca, M. G.; Silva, C. R.; Barone, J. S.; Airoldi, C. *J. Mater. Chem.* **2000**, *10*, 789. (b) Burkett, S. L.; Press: A.; Mann, S. *Chem. Mater.* **1997**, *9*, 1071.
(3) Grim, R. E. *Clay Mineralogy*, 2nd ed.; McGraw-Hill: New York, 1968.
(4) Carrado, K. A.; Thiyagarajan, P.; Winans, R. E.; Botto, R. E. *Inorg. Chem.* **1991**, *30*, 794.
(5) (a) Murray, H. H. *Clay Miner.* **1999**, *34*, 39. (b) Grim, R. E. *Applied Clay Mineralogy*; McGraw-Hill: New York, 1962.
(6) da Fonseca, M. G.; Airoldi, C. *J. Mater. Chem.* **2000**, *10*, 1457.

10.1021/cm010104o CCC: $20.00
Published on Web 09/25/2001

way to create a silane-modified clay surface is to use a postgrafting process. The reactivity of surface silanol groups toward organic molecules is exploited in this process to make organo−mineral derivatives. The types of clays that have been modified in this way include mica (a high-charge, nonswelling 2:1 phyllosilicate),[7] kaolinite,[8] and sepiolite (a fibrous clay with a tunneled structure).[9] Phenyl derivatives of sepiolite were made using this method fairly recently as well.[10]

Natural smectite clay surfaces have −OH groups only at the edges of individual particles, with their content being generally quite low, so that only limited amounts of organics can be covalently bound.[7f] The vast interlayer surface area is therefore traditionally unavailable for functionalization by this method. The new method described here, however, allows this to happen. For background information, direct grafting reactions of montmorillonite were investigated many years ago.[11] Literature regarding the surface coverage of silanes on montmorillonite clay minerals is scant, but the utility of this mineral for applications is high. One of the attractive properties is that they are converted from hydrophilic to hydrophobic when exposed to appropriate reagents. For example, octadecyltrichlorosilane ($C_{18}SiCl_3$) and octadecyltrimethoxysilane ($C_{18}Si(OMe)_3$) molecules create organic surface loadings that range from 10 to 25 wt %.[12] The effect of surface modification using these silanes on the interlayer chemistry of iron[13] and uranium[14] in a montmorillonite has been examined by X-ray absorption spectroscopy.

A wealth of other relevant organo−mineral hybrid derivatives exists in the literature. Among other layered silicates there are silane-grafted Al− and Mg−silsequioxanes[15] and magadiites.[16] Clays such as kaolinite have been postgrafted with molecules other than silanes, including methoxy groups,[17] ethylene glycol,[18] amino alcohol,[19] and phenylphosphonates.[20] Most of the recent surface modification work involves mesoporous silica materials, and using primarily silanes, the three different approaches taken are the following: (a) The silica surfaces are modified by postgrafting.[21] (b) Hybrid nanocomposites are created via direct synthesis.[22] (c) Organics are incorporated directly into the silica walls (Si−R−Si bonds) during synthesis.[23] There is a comparison of materials made via methods a and b as well.[24] An excellent review of all of these methods containing nearly 200 references was published very recently.[25]

The objective of the present study is to create a layered smectite silicate clay from a sol gel that incorporates via a one-step process an interlayer surface modified with organics via direct Si−C bonds. Organo−clays based on the hectorite structure are characterized by X-ray powder diffraction (XRD), thermal analysis, FTIR, and solid-state ^{13}C and ^{29}Si NMR. In addition, a pure inorganic hectorite was created for the first time from a tetralkoxysilane in aqueous media. TEM and nitrogen sorption data are provided as well.

Experimental Section

Materials and Methods. A general technique for the hydrothermal synthesis of smectite clay minerals in the presence of organic, organometallic, and polymeric intercalants has been developed and patented in our laboratories.[26,27] Typically the magnesium silicate clay hectorite is made because it crystallizes readily from aqueous sols. The usual silica source in this process is a silica sol. In this study, however, the silica source is replaced with an organotrialkoxysilane or tetraethoxysilane (TEOS). Conditions were optimized for an aqueous crystallization medium for ease of preparation; syntheses in methanol were unsuccessful.

The molar ratios of Si:Mg:Li in the sol gel are as given in Table 1. A slurry of 1 wt % total solids in water is made using LiF, a freshly prepared $Mg(OH)_2$ sol,[4,26,27] and the silane of choice. The silanes examined were phenyltriethoxysilane (PTES, $(C_6H_5)Si(OC_2H_5)_3$), ((methacryloxy)propyl)trimethoxysilane (MTMS, $H_2C{=}C(CH_3)COO(CH_2)_3Si(OCH_3)_3$), (3-acryloxypropyl)trimethoxysilane (ATMS, $H_2C{=}CHCOO(CH_2)_3Si(OCH_3)_3$), and tetraethoxysilane (TEOS, $Si(OC_2H_5)_4$). PTES, MTMS, and ATMS silanes were purchased from Gelest, Inc. TEOS and all other reagents were obtained from Aldrich. The purities of PTES and TEOS were determined via ^{29}Si NMR in $CDCl_3$ with 1% v/v TMS. TEOS had a single peak at −82 ppm.

(7) (a) Carson, G. A.; Granick, S. *J. Mater. Res.* **1990**, *5*, 1745. (b) Kessel, C. R.; Granick, S. *Langmuir* **1991**, *7*, 532. (c) Parker, J. L.; Cho, D. L.; Claesson, P. M. *J. Phys. Chem.* **1989**, *93*, 6121. (d) Parker, J. L.; Claesson, P. M.; Cho, D. L.; Ahlberg, A. *J. Colloid Interface Sci.* **1990**, *134*, 449. (e) Wood, J.; Sharma, R. *Langmuir* **1994**, *10*, 2307. (f) Rausell-Colom, J. A.; Serratosa, J. M. In *Chemistry of Clays and Clay Minerals*; Newman, A. C. D., Ed.; Wiley-Interscience: New York, 1987; p 371.

(8) (a) Johansson, U.; Holmgren, A.; Forsling, W.; Frost, R. L. *Clay Miner.* **1999**, *34*, 239. (b) Braggs, B.; Fornasiero, D.; Ralston, J. S.; Smart, R. *Clays Clay Miner.* **1994**, 42, *123*.

(9) (a) Ruiz-Hitzky, E.; Fripiat, J. J. *Clays Clay Miner.* **1976**, *24*, 25. (b) Fernandez-Hernandez, M. N.; Ruiz-Hitzky, E. *Clay Miner.* **1979**, *14*, 295.

(10) Aznar, A. J.; Sanz, J.; Ruiz-Hitzky, E. *Colloid Polym. Sci.* **1992**, *270*, 165.

(11) (a) Berger, G. *Chem. Week* **1941**, *38*, 42. (b) Deuel, H.; Huber, G.; Iberg, R. *Helv. Chim. Acta* **1950**, *33*, 1229. (c) Gieseking, J. E. *Adv. Agron.* **1949**, *1*, 59.

(12) Song, K.; Sandi, G. *Clays Clay Miner.* **2001**, *49*, 119.

(13) Wasserman, S. R.; Soderholm, L.; Staub, U. *Chem. Mater.* **1998**, *10*, 559.

(14) Giaquinta, D. M.; Soderholm, L.; Yuchs, S. E.; Wasserman, S. R. *Radiochim. Acta* **1997**, *76*, 113.

(15) Ukrainczyk, L.; Bellman, R. A.; Anderson, A. B. *J. Phys. Chem. B* **1997**, *101*, 531.

(16) (a) Isoda, K.; Kuroda, K.; Ogawa, M. *Chem. Mater.* **2000**, *12*, 1702. (b) Okutomo, S.; Kuroda, K.; Ogawa, M. *Appl. Clay Sci.* **1999**, *15*, 253. (c) Ogawa, M.; Miyoshi, M.; Kuroda, K. *Chem. Mater.* **1998**, *10*, 3787.

(17) (a) Komori, Y.; Enoto, H.; Takenawa, R.; Hayashi, S.; Sugahara, Y.; Kuroda, K. *Langmuir* **2000**, *16*, 5506. (b) Tunney, J. J.; Detellier, C. *J. Mater. Chem.* **1996**, *6*, 1679.

(18) (a) Tunney, J. J.; Detellier, C. *Chem. Mater.* **1993**, *5*, 747. (b) Tunney, J. J.; Detellier, C. *Clays Clay Miner.* **1994**, *42*, 552.

(19) Tunney, J. J.; Detellier, C. *Can. J. Chem.* **1997**, *75*, 1766.

(20) Guimaraes, J. L.; Peralta-Zamora, P.; Wypych, F. *J. Colloid Interface Sci.* **1998**, *206*, 281.

(21) (a) Antochshuk, V.; Jaroniec, M. *Chem. Mater.* **2000**, *12*, 2496. (b) Bu, J.; Rhee, H. *Catal. Lett.* **2000**, *66*, 245. (c) De Juan, F.; Ruiz-Hitzky, E. *Adv. Mater.* **2000**, *12*, 430. (d) Liu, A. M.; Hidajat, K.; Kawi, S.; Zhao, D. Y. *Chem. Commun.* **2000**, 1145. (e) Mokaya, R. *Angew. Chem., Int. Ed.. Engl.* **1999**, *38*, 2930. (f) Kimura, T.; Saeki, S.; Sugahara, Y.; Kuroda, K. *Langmuir* **1999**, *15*, 2794. (g) Zhao, X. S.; Lu, G. Q. *J. Phys. Chem. B* **1998**, *102*, 1556. (h) Jaroniec, C. P.; Kruk, M.; Jaroniec, M.; Sayari, A. *J. Phys. Chem. B* **1998**, *102*, 5503. (i) Liu, J.; Feng, X.; Gryxell, G. E.; Wang, L.; Kim, A. Y.; Gong, M. *Adv. Mater.* **1998**, *10*, 161.

(22) (a) Mercier, L.; Pinnavaia, T. J. *Chem. Mater.* **2000**, *12*, 188. (b) Diaz, I.; Marquez-Alverez, C.; Mohino, F.; Perez-Pariente, J.; Sastre, E. *J. Catal.* **2000**, *193*, 283. (c) Burkett, S. L.; Sims, S. D.; Mann, S. *Chem. Commun.* **1996**, 1367. (d) Macquarrie, D. J. *Chem. Commun.* **1996**, 1961.

(23) (a) Asefa, T.; Yoshima-Ishii, C.; MacLachlan, M. J.; Ozin, G. A. *J. Mater. Chem.* **2000**, *10*, 1751. (b) Asefa, T.; MacLachlan, M. J.; Coombs, N.; Ozin, G. A. *Nature* **1999**, *402*, 867. (c) Melde, B. J.; Holland, B. T.; Blanford, C. F.; Stein, A. *Chem. Mater.* **1999**, *11*, 3302. (d) Inagaki, S.; Guan, S.; Fukushima, Y.; Ohsuna, T.; Terasaki, O. *J. Am. Chem. Soc.* **1999**, *121*, 9611.

(24) Lim, M. H.; Stein, A. *Chem. Mater.* **1999**, *11*, 3285.

(25) Stein, A.; Melde, B. J.; Schroden, R. C. *Adv. Mater.* **2000**, *12*, 1403.

(26) Carrado, K. A. *Appl. Clay Sci.* **2000**, *17*, 1.

(27) Gregar, K. C.; Winans, R. E.; Botto, R. E. U.S. Patent No. 5, 308, 808, 1994.

Table 1. Synthesis Conditions for Crystallizing Silane−Hectorite Clays

silane−clay	gel molar ratio Si:Mg:Li	reacn time (days)	% hectorite[a]	elemental analysis (%) Si	Mg	Li
PTES-1	0.35:1:0.115	5	100	19.1	9.42	0.71
PTES-2	0.7:1:0.115	5	90[b]	18.7	6.71	0.77
TEOS-1	0.4:1: 0.115	2	100	22.6	15.1	0.52
TEOS-2	0.5:1:0.25	2	100	23.4	14.6	0.86
MTMS-1	1.5:1:0.115	4	50	nd[c]	nd	nd
MTMS-2	0.75:1:0.115	2−4	25	nd	nd	nd
ATMS	0.75:1:0.115	4	25	nd	nd	nd

[a] Determined using XRD and IR as discussed in text. [b] Determined from TGA (388 °C $Mg(OH)_2$ impurity peak in Figure 3b). [c] nd = not determined.

PTES had two peaks at −57.6 ppm (98.15%) with a slight impurity at −48.5 ppm (1.85%). To make the clay, LiF is slurried in water and the $Mg(OH)_2$ sol is added. This mixture is stirred for 30 min, the silane is added, and the volume is brought to 100 mL. The slurries are refluxed for 2−5 days and then centrifuged, washed, and air-dried. The reaction did not go as far toward completion at room temperature as it did at reflux temperature. Throughout the course of the reaction the pH = 8.5−9. The PTES−hectorites were heated very slowly at the beginning and were also exhaustively washed to remove impurities.

Characterization. XRD analyses were carried out on a Rigaku Miniflex+ instrument using Cu Kα radiation, a fixed power source (30 kV, 15 mA), a NaI detector, variable slits, a 0.05° step size, and a 0.50° 2θ/min scan rate. Powders were loosely packed in horizontally held trays. TGA-DTA (thermal gravimetric analysis and differential thermal analysis) measurements were obtained either on a SDT 2960 from TA Instruments or a Seiko ExStar TG/DTA 6200 from Haake Instruments. For these samples, measured against an alumina standard in a 100 mL/min O_2 flow with a temperature ramp of 10 °C/min to 800 °C, no major differences were observed between TGA and DTA. Total organic loadings were calculated by measuring the weight loss over the appropriate temperature range, which compared favorably with the % C determined via microanalysis. A LECO CHN-900 analyzer was used to determine % C (combustion at 1000 °C, detection limit of 0.05 wt % C, calibrated with calcium oxalate). The IR measurements were made on a Nicolet 510P FTIR using KBr pellets and a resolution of 2 cm^{-1}.

The solid-state ^{13}C and ^{29}Si nuclear magnetic resonance spectra were recorded at 4.70 T (50.3 MHz for ^{13}C and 39.8 MHz for ^{29}Si) on a Bruker Avance DSX-200 spectrometer. The samples were packed into a 300-μL ceramic rotor and spun at 7000 ± 2 Hz in a Bruker 7 mm MAS probe. Carbon spectra were recorded with the cross-polarization pulse sequence, 2 ms contact time, 6.4 μs 90 ° pulse, 3 s recycle delay, 4000 transients, and a 20 kHz sweep width. Silicon spectra were recorded with the standard Bloch decay experiment, 7.0 μs 90° pulse, 200 s recycle delay, 312 transients, and 20 kHz sweep width. All data were acquired in the presence of proton decoupling with proton power set to 80 kHz. For all spectra, the 2k words of memory allocated for data acquisition were zero filled to 8k words and multiplied by an exponential function (20 Hz for carbon and 40 Hz for silicon) prior to Fourier transform. Chemical shift data are with respect to TMS. Hexamethylbenzene was used as a secondary reference for ^{13}C spectra, and TKS was used as a secondary reference for ^{29}Si spectra.[28]

Specimens for transmission electron microscopy (TEM) were imaged in a JEOL 100CXII instrument operating at 100 kV in the Electron Microscopy Collaborative Research Center at Argonne National Laboratory. Powder samples of clay were dispersed in methanol and sonicated for 30 s, and 1−2 drops were placed onto "holey" carbon films supported on copper grids. These specimens were allowed to air-dry followed by a vacuum oven heating to 100 °C for 2 h. Bright-field TEM images are shown in Figure 9; selected area electron diffraction patterns are included as insets.

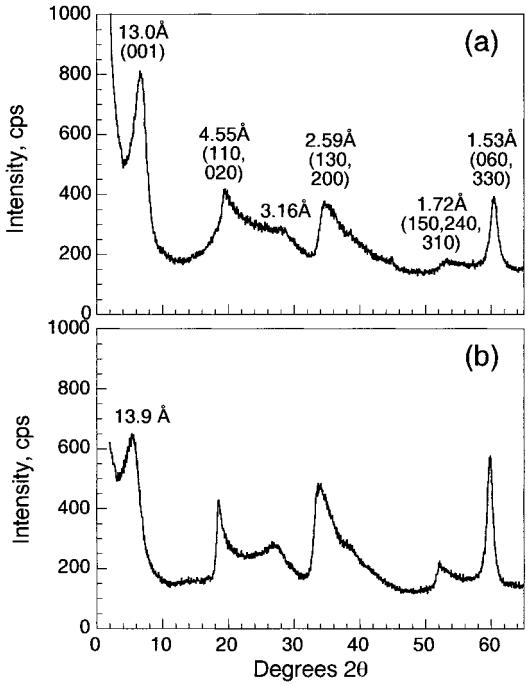

Figure 2. X-ray diffraction patterns of (a) PTES-1, a synthetic phenyl−hectorite clay derived from phenyltriethoxysilane, and (b) TEOS-1 hectorite derived from tetraethoxysilane.

Some nitrogen sorption isotherms were collected on a Quantachrome Autosorb-6 instrument. About 0.10 g of material was weighed into a Pyrex sample tube and evacuated to 80 mTorr overnight at RT and then backfilled with He. The static physisorption experiments measured the amount of nitrogen adsorbed or desorbed at liquid-nitrogen temperature as a function of pressure (P/P_0 = 0.025−0.999). Other sorption data were obtained using a Micromiretics ASAP 2010; about 0.10 g of sample was degassed for 3 h at RT and then 2 h at 110 °C.

Results and Discussion

XRD and Thermal Analysis. Table 1 presents synthesis conditions and the relative degrees of success in isolating silane−clay products. Incomplete crystallization is indicated by the presence of peaks, to various degrees, for starting material $Mg(OH)_2$ in XRD and IR. Using this as a guide, a ranking of the silanes in terms of their synthetic success is PTES = TEOS > MTMS ≥ ATMS.

Figure 2 displays XRD patterns for a silane-prepared clay, in this case PTES, and for the hectorite made using TEOS. In these patterns all of the expected peaks for hectorite are present and at the same time there are no peaks due to $Mg(OH)_2$ (the mineral brucite). Peak assignments are indicated on the figure; the peak at about 3.16 Å may be a higher order (004) reflection of the basal spacing.

Figure 3 shows the TGA weight loss and first derivative traces for PTES-1 and -2. The first peak occurring near 100 °C is due to adsorbed surface water. A typical synthetic hectorite clay without any organic does not show another noticeable weight loss event until dehydroxylation at about 800 °C.[29] There is significant

(28) Muntean, J. V.; Stock, L. M.; Botto, R. E. *J. Magn. Reson.* **1988**, *76*, 540.

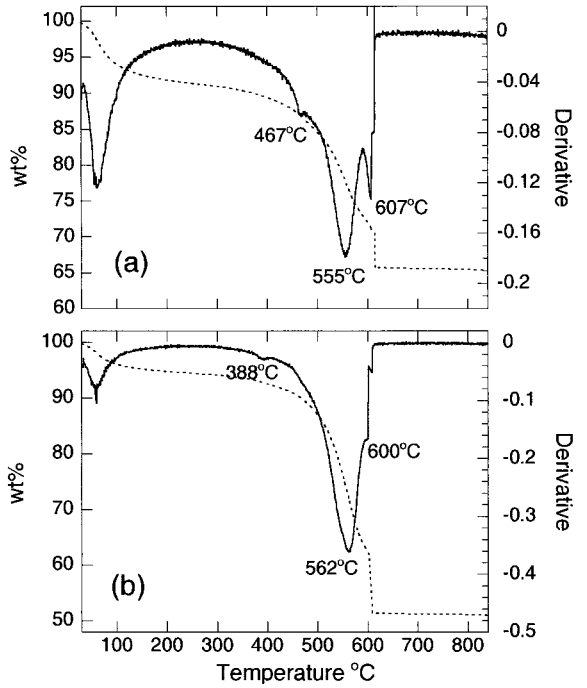

Figure 3. TGA data for (a) PTES-1 and (b) PTES-2 hectorites as described in Table 1. Percent weight loss (dashed line) is given on the left axis, and the derivative of the weight loss curve (solid line) is given on the right.

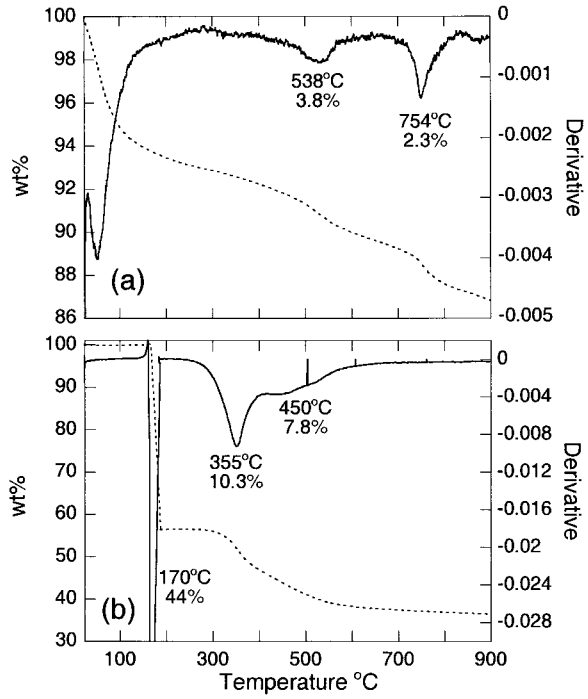

Figure 4. TGA data for (a) TEOS-1 and (b) MTMS-1 hectorites as described in Table 1. Percent weight loss (dashed line) is given on the left axis, and the derivative of the weight loss curve (solid line) is given on the right.

weight loss between these two regions in the PTES samples. This is typical for organo−clays, and it can be used as an indication of how much organic is loaded onto the clay.[29,30] The feature at 388 °C for PTES-2 (Figure 3b) can be assigned to unreacted $Mg(OH)_2$ in this matrix.[29] Interestingly, the dehydroxylation event for these samples is either greater than 850 °C or else it has destabilized significantly to 600 °C. This is an indication that something has indeed modified the clay structure in some way. Using TGA alone there is no way to determine exactly what is causing the sharp, exothermic event at 600 °C. Figure 4 shows the TGA data for TEOS-1 and MTMS-1. Using the rationale described above, the peak at 538 °C in TEOS-1 is assigned to organic (3.8 wt %) and the 754 °C peak is assigned to clay lattice dehydroxylation. It is assumed that the small amount of organic present in TEOS-1 is due to adsorbed residual ethanol from the alkyoxysilane hydrolysis. The mixed-phase MTMS-1 sample in Figure 4b is provided for comparison purposes only.

Table 2 summarizes physical characterization data including XRD, TGA and nitrogen sorption measurements. Basal spacings, or the *d*(001) reflection along the *c* axis, include the height of a 2:1 clay unit (9.6 Å for natural smectites) plus the interlayer space. The 13.0 Å basal spacing for PTES-1 therefore yields an interlayer height of 3.4 Å. The large amount of organic in the PTES−hectorites (25% and 41% respectively for PTES-1 and -2) is likely creating a hydrophobic environment that would exclude excess water. Indeed, PTES-1 contains only about 7 wt % water (<120 °C wt loss in TGA). The size of a benzene molecule has been calculated at 6.6 × 7.3 × 3.3 Å using van der Waals radii.[31]

Table 2. Physical Characterization Data for Various Synthetic Silane−Hectorite Clays

silane−clay	XRD *d*(001), Å	% C[a]	wt loss[b] 400−800 °C	surf area,[c] m^2/g	pore vol,[c] cm^3/g
PTES-1	13.0	19.86	25.4	233	0.25
PTES-2	13.0	31.37	40.8	nd[e]	nd
TEOS-1	13.9	0.58	3.8	321	0.22
MTMS-1	15.1	nd	18.1[d]	nd	nd

[a] Determined via microanalysis. [b] Determined via TGA. [c] N_2 BET method. [d] 300−800 °C; sample also had 44 wt % loss at 170 °C. [e] nd = not determined.

These dimensions lead one to believe that the pendant phenyl groups from PTES (the triethoxy groups are assumed to be hydrolyzed away) are actually lying flat within the interlayer. This is a high energy arrangement considering the orientation of the Si−C bond. However, the spacing is significantly higher than that reported for the similarly prepared PTES−talc (11.8 Å)[2b] and, therefore, assumed to be that much more favorable. Further evidence that this silane-derived hectorite is organo-grafted and not just a mixture of products such as hectorite and unreacted PTES, for example, is that the basal spacing is different from similarly prepared hectorites without silane present. Specifically, the pure synthetic hectorite made via the same procedure but with silica sol as the silicon source rather than an organosilane has a basal spacing of 15.0 Å and contains about 16 wt % water.[30] In this material, the exchangeable cations are hydrated Li(I) ions and the large amount of water causes the clay to swell and subsequently increase the basal spacing. Li(I) cations are also the exchangeable cations in PTES-1, but there is less water present to swell the layers.

(29) Carrado, K. A.; Thiyagarajan, P.; Song, K. *Clay Miner.* **1997**, *32*, 29.
(30) Carrado, K. A. *Ind. Eng. Chem. Res.* **1992**, *31*, 1654.
(31) Webster, C. E.; Drago, R. S.; Zerner, M. C. *J. Am. Chem. Soc.* **1998**, *120*, 5509.

In TEOS−hectorite the low amount of organic at 3.8 wt % is not surprising considering the reactivity of the alkoxy groups to hydrolysis and is presumed to be due to residual ethanol. It is difficult to determine the amount of organic in the incompletely formed MTMS−hectorites because of its mixed phase nature (both clay and brucite are seen in XRD). The first peak at 170 °C accounts for a 44% weight loss and is highly exothermic with a DTA signal of 2500 μV. For comparison, a C8-alkylated silica gel showed similar behavior with an exothermic flash at 200 °C. The flashpoint of pure MTMS is 92 °C. Whether the MTMS is bound to a condensed silica phase, brucite, or clay, and in what ratios, is unclear from these data.

Elemental Analysis. The percents by weight of Si, Mg, and Li of PTES− and TEOS−hectorites are provided in Table 1. By a calculation that assumes an ideal hectorite composition with every silicon atom bonded to a phenyl group, a structural formula of $Li_{1.32}Si_8Mg_{5.34}(OH,F)_4O_{12}(C_6H_5)_8 \cdot 6.3H_2O$ (using the 8% water that is observed by TGA) would contain a theoretical amount of 43% phenyl by weight. The actual loading is only 21.24% phenyl, however, as calculated from the 19.86% C microanalysis result. This corresponds to a composition of $Li_{1.32}Si_8Mg_{5.34}(OH,F)_4O_{16.08}(C_6H_5)_{3.92} \cdot 4.8H_2O$. The calculated amounts from this latter formula are 20.9 wt % Si, 12.1 wt % Mg, and 0.86 wt % Li (Si/Mg = 1.7). The actual values are close at 19.1 wt % Si, 9.42 wt % Mg, and 0.71 wt % Li (Si/Mg = 2.0). (The calculated values for the fully grafted material are 15.8 wt % Si, 9.1 wt % Mg, and 0.65 wt % Li.)

Assuming an ideal hectorite composition and 7 wt % H_2O (determined from TGA) for the TEOS samples, the molecular formula of TEOS-*n* should be $[Li_{.66}Si_8(Mg_{5.34}\ Li_{.66})O_{20}(OH,F)_4] \cdot 3.1H_2O$. This yields calculated values of 27.8 wt % Si, 16.1 wt % Mg, and 1.14 wt % Li (Si/Mg = 1.7). TEOS-1 has actual values of 22.6 wt % Si, 15.1 wt % Mg, and 0.52 wt % Li (Si/Mg = 1.5). For TEOS-2, in which the gel contained slightly more Si and Li, theses values increase to 23.4 wt % Si and 0.86 wt % Li, with 14.6 wt % Mg (Si/Mg = 1.6).

IR Studies. Figure 5 and Table 3 present IR data for PTES-1 hectorite. Figure 5a shows the entire spectrum from 4000 to 400 cm^{-1}, while Figure 5b expands the midregion from 3200 to 1200 cm^{-1}. Assignments are made in Table 3, and all peaks can be attributed to either the clay structure (including adsorbed water) or organic.[32] The organic peaks correspond primarily to aromatics and even more specifically to a monosubstituted aromatic as would be expected from a phenyl-grafted clay. There is a very small contribution from aliphatic carbon indicated in the IR as well. The sharp peak at 1431 cm^{-1} has been assigned to the Si−C_6H_5 moiety of the PTES−talc version of this organic−inorganic synthetic hybrid[2b] and to the Si−C unit of similar aminosilane-derived grafted talcs.[1a] This peak has been reported, but not assigned, for various natural clay−aromatic complexes.[33]

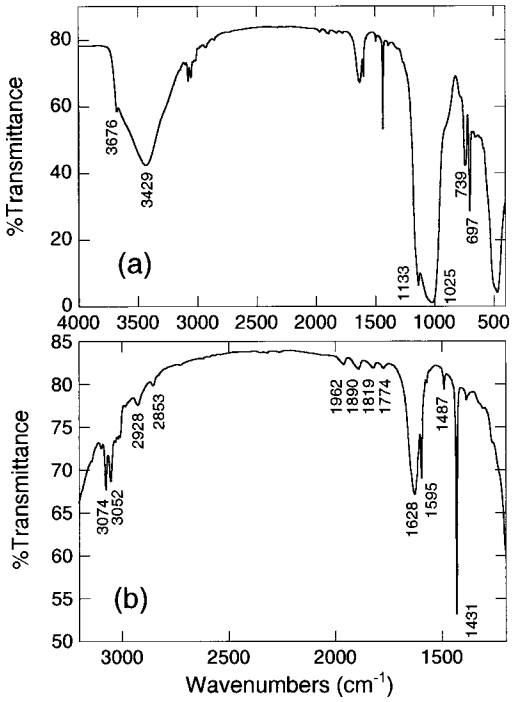

Figure 5. IR spectra PTES-1 (synthetic phenyl−hectorite) over (a) the entire range and (b) the 1200−3200 cm^{-1} range as an expanded view. See Table 3 for assignments.

Table 3. Assignments of IR Bands for Synthetic Hectorites in Figures 5 and 6

assgnt	PTES-1, cm^{-1}	TEOS-1, cm^{-1}
clay struct hydroxyl O−H str	3676	3679
adsorbed water, H-bonding, O−H str	3429	3435
aromatic C−H str	3074, 3052	na[b]
aliphatic C−H str	2928, 2853	2929
monosubstituted benzene overtones	1962, 1890, 1819, 1774	na
adsorbed water, O−H bend	1628	1633
aromatic C=C ring str	1595, 1487	na
Si−aromatic[a]	1431	na
aliphatic C−H bends	1430, 1383	
Si−O str	1133	
Si−O−Si str	1025	1021
monosubstituted benzene oop bends	739, 697	na
adsorbed water, O−H bend	663	

[a] See discussion. [b] na = not applicable.

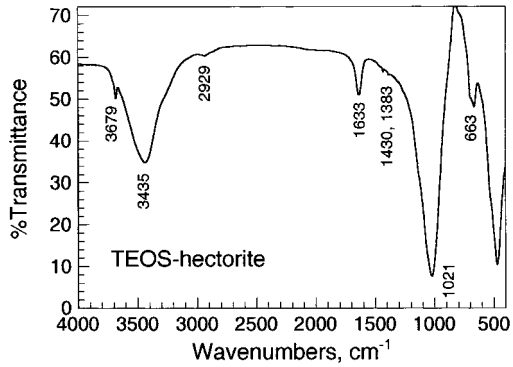

Figure 6. IR spectrum of TEOS-1 hectorite. See Table 3 for assignments.

The IR spectrum for TEOS-1 hectorite is shown in Figure 6 with assignments in Table 3, and it is comparatively much simpler than the PTES-1 data. As indicated in the TGA results, only a small amount of

(32) (a) Berry, F. J.; Hayes, M. H. B.; Jones, S. L. *Inorg. Chim. Acta* **1990**, *178*, 203. (b) Farmer, V. C. In *Data Handbook for Clay Minerals and Other Non-Metallic Minerals*; Van Olphen, H., Fripiat, J. J., Eds.; Pergamon Press: New York, 1979; p 285. (c) Pavia, D. L.; Lampman, G. M.; Kriz, G. S. *Introduction to Spectroscopy*; Saunders Co.: Philadelphia, PA, 1979; p 13.

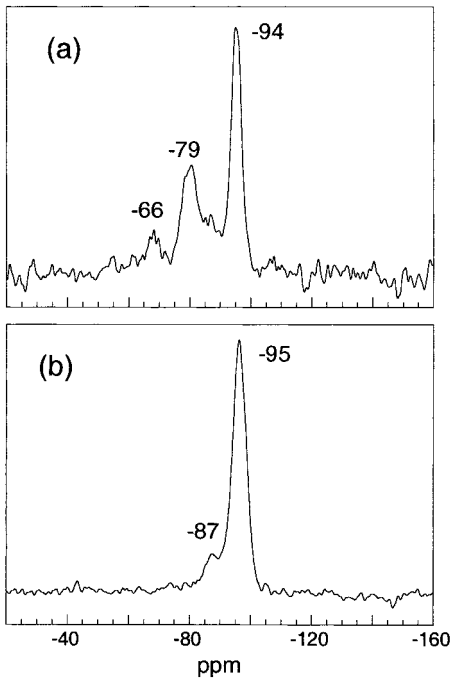

Figure 7. Solid-state ^{29}Si NMR spectra of (a) PTES-1 (synthetic phenyl−hectorite) and (b) synthetic TEOS-1 hectorite.

organic is associated with this sample (4 wt %) and therefore there is only a minor presence of organic indicated in the IR. Note that only one Si−O stretch is observed in the IR for TEOS−hectorite at 1021 cm^{-1}, which corresponds specifically to the Si−O−Si stretch.[31a,b] PTES-1 shows an additional peak in this region at 1133 cm^{-1}. For the similarly prepared PTES−talc grafted material,[2b] the peak at 1120−1150 cm^{-1} was assigned to R−Si−O. Since the TEOS−hectorite displays only one band in the Si−O region, PTES-1 displays two, and the only difference between them is the grafted organic group, it is reasonable to assign this band to R−Si−O. As a caveat however, note that most other hectorites (whether synthetic or natural)[29,32a,b] also have another peak at slightly higher frequency that is assigned to a simple Si−O stretch.

Both TEOS-1 and PTES-1 samples also show a small sharp peak at 3676−3679 cm^{-1} that is due to the clay−OH hydroxyl band.[29] The Mg−OH hydroxyl band of brucite would occur at 3700 cm^{-1} if it were present.[29] As with XRD results, there is no evidence that any unreacted, uncondensed brucite starting material exists for these particular samples. When the reaction is not complete, as in PTES-2 (data not shown) and other mixed-phase samples, a weak sharp peak at 3700 cm^{-1} is indeed observed.

NMR Studies. Figure 7 shows the ^{29}Si NMR spectra for PTES-1 and TEOS-1 hectorites. The most intense peak at −94 ppm for PTES-1 (Figure 7a) is assigned to the tetrahedral Q3(0Al) Si*(OMg)$(OSi)_3$ site reported previously at −94 to −95 ppm for natural hectorites,[34] at −94 ppm for synthetic hectorite made using silica sol,[35] and at −94.4 ppm for the synthetic hectorite called Laponite.[32a] The term Q3 refers to the number of branching units typical of sheet silicate structures, and (0Al) indicates that no aluminum is present to affect the chemical shift (the presence of aluminum is ubiquitous in most natural sheet silicates). Note that no higher field peaks exist for the Q4 tetrafunctional Si$(OSi)_4$ units typical of colloidal silica sol, for instance, −107 ppm for Ludox HS-40.[36] There are instead lower field peaks. These occur at −79 and −66 ppm and have been assigned to RSi*(OMg)$(OSi)_2$ and RSi*(OMg)(OSi)-(OH) species, respectively, in the analogous PTES−talc, phenyl-grafted synthetic material[2b] (at −78 and −70 ppm).

The ^{29}Si NMR spectrum for TEOS-1 hectorite (Figure 7b) is dominated by the single Q3 Si*(OMg)$(OSi)_3$ hectorite clay peak at −95 ppm. There is an additional small contribution at −87 ppm for which assignment becomes somewhat challenging. Signals for RSi*(OMg)-$(OSi)_x(OH)_y$ species are of course not expected because TEOS does not have an R−Si bond. Also, the amount of organic is quite low (3.8%), and ^{13}C NMR revealed essentially no signal (data not shown). The chemical shift for a Si*$(OSi)_2(OH)_2$ species has been reported at −89 ppm.[37] A peak at −85 ppm has been observed in silica sols as the particle size decreases and assigned to a Q2 branching species that contains two hydroxyl groups.[35] Synthetic hectorites made from a silica sol also show evidence of this peak at −85 ppm to some degree, especially at intermediate crystallization times.[34] This peak is therefore assigned to either an incompletely condensed Si*(OMg)$(OSi)_2$(OH) unit or to a Si*$(OSi)_2$-$(OH)_2$ species.

Silanol-containing groups such as RSi(OMg)(OSi)(OH) are not entirely unexpected in these systems. In fact, large amounts of RSi(OMg)(OSi)(OH) and RSi(OMg)-$(OH)_2$ species are observed in the synthetic organo-grafted talc derivatives reported previously.[1b,2] They have been assigned to partially condensed silicon species due to geometric constraints during packing, slow condensation kinetics, or edge sites in samples with small particle size [for RSi(OMg)(OSi)(OH) species].[1b,2b] In those materials, there was no evidence of the four oxygen-bridged Si centers that are typical of smectites (Q3) and that occur in PTES-1. If the assignments are correct, then in the aqueous hectorite clay gel reported here it is apparent that some of the PTES silane starting material is hydrolyzing at the normally quite stable Si−C linkage. This is an unusual and unexpected result, and it does not occur in the PTES−methanol solutions used to prepare the talc derivatives. The Si−C linkage is quite strong and not prone to typical hydrolysis. But the supposition is consistent with the elemental analysis and TGA results as well. Further research into the specific conditions (pH, temperature, reactants, etc.) that might be causing this is certainly warranted.

(33) (a) Johnston, C. T.; Tipton, T.; Stone, D. A.; Erickson, C.; Trabue, S. L. *Langmuir* **1991**, *7*, 289. (b) Berry, F. J.; Hayes, M. H. B.; Jones, S. L. *Inorg. Chim. Acta* **1990**, *178*, 203. (c) Fenn, D. B.; Mortland, M. M.; Pinnavaia, T. J. *Clays Clay Miner.* **1973**, *21*, 315.

(34) (a) Komarneni, S.; Fyfe, C. A.; Kennedy, G. J.; Strobl, H. *J. Am. Ceram. Soc.* **1986**, *69*, C45. (b) Weiss, C. A.; Altaner, S. P.; Kirkpatrick, R. J. *Am. Miner.* **1987**, *72*, 935. (c) Kinsey, R. A.; Kirkpatrick, R. J.; Hower, J.; Smith, K. A.; Oldfield, E. *Am. Miner.* **1985**, *70*, 537.

(35) Carrado, K. A.; Xu, L.; Gregory, D. M.; Song, K.; Seifert, S.; Botto, R. E. *Chem. Mater.* **2000**, *12*, 3052.

(36) Ramsay, J. D. F.; Swanton, S. W.; Matsumoto, A.; Goberdhan, D. G. C. In *The Colloid Chemistry of Silica*; Bergna, H. E., Ed.; Advances in Chemistry Series 234; American Chemical Society: Washington, DC, 1994; p 67.

(37) Sindorf, D. W.; Maciel, G. E. *J. Am. Chem. Soc.* **1983**, *105*, 3767.

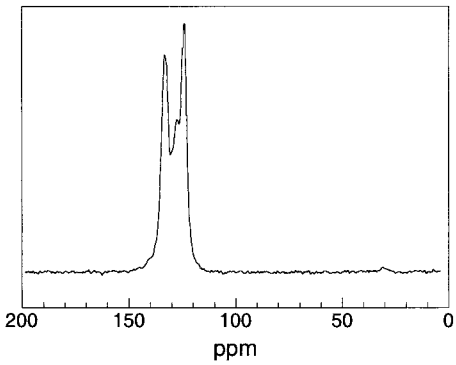

Figure 8. Solid-state ^{13}C NMR spectrum of PTES-1 (synthetic phenyl−hectorite).

Finally, note again that there is no signal near −112 ppm due to Q4 tetrafunctional Si−O groups such as seen in silica gels or sols.

A fully grafted material wherein every silicon is bonded to a phenyl group would necessitate that the completely condensed basal oxygen surface typical of clays would not occur. The fact that no Q3 clay signal is observed in the Si NMR of PTES−talc materials and that the basal spacings are quite low at 11.8 Å may mean that the phenyl groups bonded to silicon lie much more within what would ordinarily be the basal oxygen plane. The PTES−hectorite material may then be a hybrid between these two end-members, containing some of the Q3 basal oxygen character of clays along with Si−phenyl groups lying to a lesser degree within that plane. This follows since the basal spacing is higher at 13.0 Å and only about half of the silicon atoms remain grafted to organic.

Figure 8 shows the solid-state ^{13}C NMR spectrum for PTES-1. Resonances occur at 128.2, 130.5, and 134.5 ppm and comprise the shifts expected for the monosubstituted phenyl group of PTES-1 hectorite. For the synthetic phenyl−talc derivative these peaks occurred at 127.8, 130.5, and 134.1 ppm.[2b] In neither case was resolution of the Si−C carbon observed (expected at 131 ppm) due to either insufficient CP combined with a long relaxation time for this particular carbon or else it is simply obscured by the fairly broad resonances nearby.[2b] The phenyl resonances are indeed noticeably broadened, which is indicative of immobilized organic groups.[1b,2a] Immobilization within the 3.4 Å interlayer gallery space is entirely expected.

TEM Data. TEM images of PTES-1, PTES-2, and TEOS-1 hectorites are provided in Figure 9. The morphologies observed are typical of the smectite clay structure, with large stacked plates that are flexible enough the curl at the edges. PTES-2 appears to have smaller plates that result in a morphology that is, overall, more open. The electron diffraction pattern insets clearly show rings for clay in the case of TEOS; these are slightly more diffuse in the case of PTES-1 and difficult to resolve at all in the case of PTES-2.

Sorption Data. Nitrogen sorption isotherms for PTES-1 and TEOS-1 hectorites are shown in Figure 10. Because of the presence of hysteresis loops between adsorption and desorption branches, these isotherms are classified as type IV.[38] The TEOS-1 hectorite has a type H2 hysteresis loop, which is difficult to interpret and is vaguely attributed to mesoporous networks of "broad"

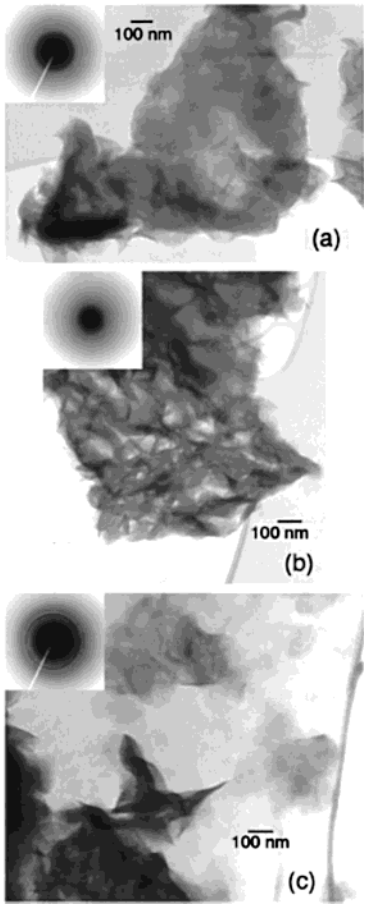

Figure 9. TEMs of (a) PTES-1, (b) PTES-2, and (c) TEOS-1 hectorites.

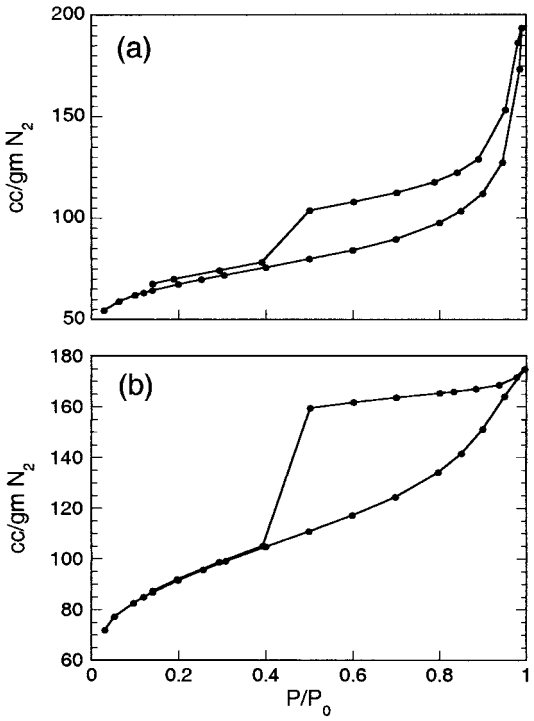

Figure 10. Nitrogen sorption isotherms for (a) PTES-1 and (b) TEOS-1 hectorites (bottom traces, adsorption; top traces, desorption).

structure.[38] Interestingly, the shape is similar to those of synthetic hectorites made using the same procedure

but with silica sol as the silicon source.[39] Type H3 hysteresis is observed for PTES-hectorite, and it is entirely typical of clay, being attributed to aggregates of platelike particles giving rise to slit-shaped pores.[38] In all cases the desorption branch shows an inflection "knee" at about 0.45−0.5 P/P_0. This gives rise to a sharp peak at 37−39 Å in the desorption pore size distributions that has been observed for many different types of layered materials when using nitrogen as the sorbent gas; it is an artifact of the desorption process when using nitrogen and is therefore ignored.[40] Generally the specific surface areas from type IV isotherms are quite reliable,[37] and these data are summarized in Table 2.

Conclusions

The mechanism of formation of the PTES− and TEOS−hectorites is apparently different from that proposed by Mann and co-workers[1b,2b] for organo-grafted talc derivatives. In the latter case, the octahedral MgO layer is condensing at the same time as Si−O species are bonding. This allows for high degrees of organosilane incorporation, but it also causes distortions, puckering, and incomplete condensation toward a typical smectite clay lattice. In the case of the grafted hectorites reported here, it is more likely that silicate/silane species are grafting to the preexisting $Mg(OH)_2$ brucitic sheets. This mechanism of formation should be similar to one proposed recently for the crystallization of hectorite.[34] The choice of silane and the degree of crystallization success are apparently highly dependent upon the use of an aqueous medium for hectorite formation in this process. The synthetic phenyl−hectorite, for example, disperses again in water after isolation. The ATMS and MTMS silanes are less successful in forming pure clay products, and this might be a result of their difference in reactivity in aqueous media versus PTES. Of interest next will be reactivity of the phenyl groups in materials such as PTES-1 to reactions such as nitration and sulfonation similar to the phenyl derivatives created from grafted sepiolites.[10] In addition, the option of ion-exchangeability is added in the hectorite clay system that is not available to the synthetic talc analogues. This allows for the presence of counterions other than the simple Li(I) cation used here.

Natural smectite clay surfaces have −OH groups only at the edges of individual particles, with their content being generally quite low, so that only limited amounts of organics can be covalently bound.[7f] The vast interlayer surface area is therefore traditionally unavailable for functionalization by a postgrafting method. The new method described here, however, allows for more grafting both because it is an in situ process and because there are more Si−OH silanol groups present. Finally, it is important to note that a pure synthetic hectorite can be made using the hydrothermal crystallization method with TEOS rather than silica sol as the silicon source.

Acknowledgment. R. Botto assisted in the design of the NMR experiments, C. Bloomquist performed the IR measurements, and S. Macha performed some of the sorption measurements and the alkylated silica gel TGA standards (all CHM ANL). A. Essling and S. Lopykinski performed the % Si, Mg, Li analysis using ICP-AES, and L. Tenkate performed the % C microanalysis (all of the Analytical Chemistry Lab, ANL). The input of the reviewers of this manuscript is greatly appreciated. This research was performed under the auspices of the U.S. Department of Energy, Office of Basic Energy Sciences, Divisions of Chemical Sciences (K.A.C., L.X., J.V.M.) and Materials Science (R.C.) under Contract No. W-31-109-ENG-38.

CM010104O

(38) Sing, K. S. W.; Everett, D. H.; Haul, R. A. W.; Moscou, L.; Pierotti, R. A.; Rouquerol, J.; Siemieniewska, T. *Pure Appl. Chem*. **1985**, *57*, 603.

(39) Carrado, K. A.; Csencsits, R. *Prepr. Pap.—Am. Chem. Soc., Div. Petrol. Chem*. **2001**, *46*, 48.

(40) Everett, D. H. In *Characterization of Porous Solids*; Gregg, S. J., Sing, K. S. W., Stoeckli, H. F., Eds.; Society of Chemistry and Industry: London, 1979; pp 253 and 299.